
**Journal of Macromolecular Science, Part A**
Publication details, including instructions for authors and subscription information:
http://www.informaworld.com/smpp/title~content=t713597274

# Fourier-Transform Infrared Photoacoustic Spectroscopy of Synthetic Polymers

B. Jasse[a]
[a] Laboratoire de Physicochimie Structural et Macromoléculaire, Ecole Supérieure de Physique et de Chimie de Paris 10, PARIS Cedex 05, France

**To cite this Article** Jasse, B.(1989) 'Fourier-Transform Infrared Photoacoustic Spectroscopy of Synthetic Polymers', Journal of Macromolecular Science, Part A, 26: 1, 43 — 67
**To link to this Article: DOI:** 10.1080/00222338908053843
**URL:** http://dx.doi.org/10.1080/00222338908053843

J. MACROMOL. SCI.–CHEM., A26(1), pp. 43-67 (1989)

# FOURIER-TRANSFORM INFRARED PHOTOACOUSTIC SPECTROSCOPY OF SYNTHETIC POLYMERS

B. JASSE

Laboratoire de Physicochimie Structurale et Macromoléculaire
Ecole Supérieure de Physique et de Chimie de Paris
10, rue Vauquelin, 75231 PARIS Cedex 05, France



## ABSTRACT

Although not yet widely used in analytical laboratories, the tremendous development of low-cost FTIR spectrometers should allow photoacoustic spectroscopy to become a commonly used technique for polymer analysis. The ability to determine depth profiles in a broader range than ATR makes FTIR-PAS a particularly attractive method to follow the effect of chemical treatments or the penetration of coatings in polymeric materials. The possibility to obtain a spectrum from as-received samples is also of great interest to the analytical chemist. The only limitation of this technique is the need to use a great number of scans to enhance the signal-to-noise ration. However, continued improvements in PA cell design should increase the overall sensitivity, leading to shorter data-collection times.

## I. INTRODUCTION

The photoacoustic effect was accidently discovered by Alexander Graham Bell [1] in 1880, who observed that thin diaphragms emitted sounds when illuminated by modulated sunlight. In his experiments [2], a sample was placed in a brass cavity closed by a glass window. A brass tube was used to conduct the sound to the ear. The samples that produced the loudest sounds were those that had the darkest color or which were of a loose or porous nature. Due to the lack of sensitive sound detectors and high-power light

sources, the photoacoustic effect was to remain unexplored until Rosencwaig [3] presented the first nonresonant photoacoustic cell.

In 1975, UV-visible photoacoustic spectroscopy (PAS) became an available commercial technique and found various applications in the analysis of solid samples. The use of PAS in the mid-infrared region is also of great interest for the chemical and physical analysis of solid samples. The development of Fourier-transform infrared spectroscopy (FTIR), with its throughput and multiplex advantages, allowed the coupling of FTIR and PAS. The first polymer PAS spectrum (polystyrene) (PS) was published in 1979 by Rockley [4] in the 1000-400 $cm^{-1}$ range and is reproduced in Fig. 1. Although the spectrum obtained was quite noisy, the general features of the aromatic and aliphatic C–H stretching at 2800-3100 $cm^{-1}$ are clearly visible. The next year, Rockley [5] presented spectra corrected for atmospheric $H_2O$ and $CO_2$ vapors by the use of an activated charcoal reference spectrum, and Vidrine [6] published the spectra of other polymeric compounds. Since these pioneer publications, FTIR-PAS has been used to study different polymer systems. The aim of the present paper is to give an overview of the PAS technique and to focus on recent significant developments in FTIR-PAS in the synthetic polymer field. For an overview of FTIR-PAS, the reader is referred to the review articles by Vidrine and Lowry [7], Koenig [8], and Graham, Grim, and Fateley [9].



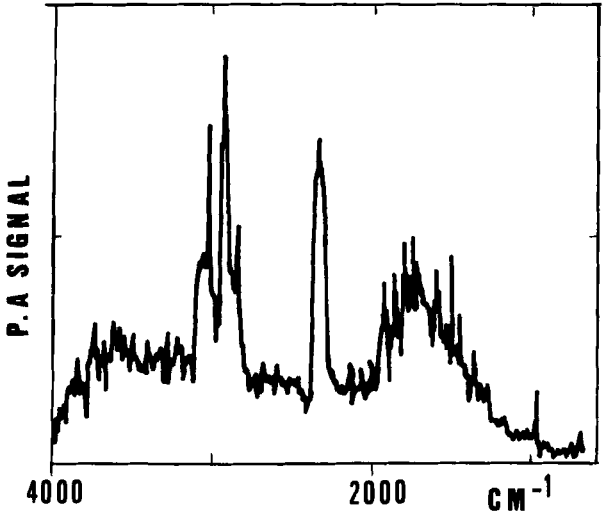


FIG. 1. PA spectrum of a polystyrene film (from Ref. 4).

## II. THEORETICAL BACKGROUND

In an FTIR-PAS experiment, radiation from a midrange IR source is modulated by the moving mirror of an interferometer. The modulated radiation is then focused onto the sample which is placed inside a cell filled with an IR-transparent gas and fitted with a microphone (Fig. 2). On penetrating the sample, the incident radiation is selectively absorbed, depending on the value of the optical absorption coefficient of the sample, $\beta$. The absorbed energy is lost as heat through nonradiative processes. Because the incident radiation is modulated, the temperature rise is periodic at the modulation frequency, and it is this periodic temperature rise at the surface of the sample which induces a corresponding pressure change of the gas in the cell. This pressure modulation is an acoustic signal which is detected by the microphone and then electronically converted to a voltage.

The quantitative aspect of the photoacoustic (PA) effect has been treated by Rosencwaig and Gersho [10] on the basis of a one-dimensional analysis



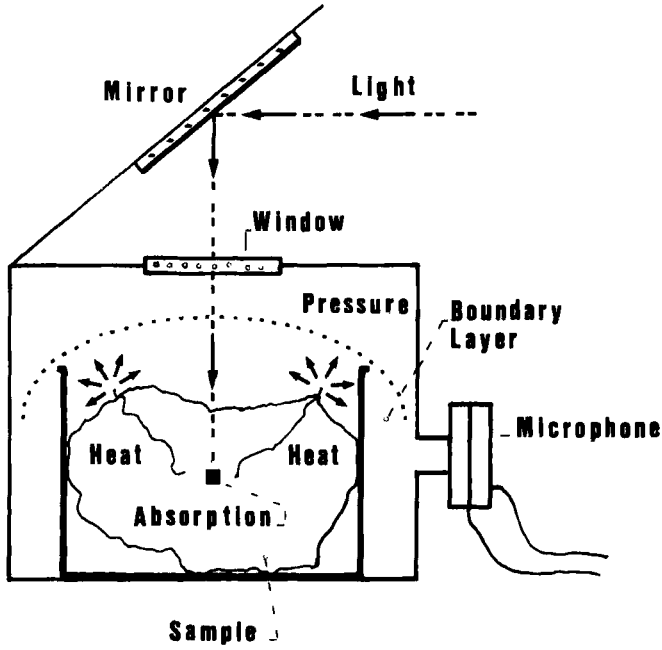


FIG. 2. Schematic representation of a PA cell.

of the production of a photoacoustic signal in a simple cylindrical cell. Further refinements of the Rosencwaig-Gersho theory have been made [9]. In this review we only give an overview of the Rosencwaig-Gersho theory. For a more in-depth treatment, the reader is referred to Rosencwaig's book [11].

The intensity of the modulated infrared beam coming from the interferometer varies sinusoidally and is given by

$$I = \frac{1}{2} I_0 (1 + \cos 2\pi\omega t),$$

where $I_0$ is the intensity of the incident light of wavelength $\lambda$, and $\omega$ is the modulation rate in cycles per second. We let $\beta$ (in $\mathrm{cm}^{-1}$) denote the optical absorption coefficient of the solid sample for wavelength $\lambda$. Because the absorption of light is an exponential process, the heat density generated at any point $x$ in the solid sample is then given by

$$\frac{1}{2} \beta I_0 e^{\beta x} (1 + \cos 2\pi\omega t).$$

The thermal diffusion length $\mu$ (in cm) is a measure of the generated heat which is able to reach the surface of the sample. The value of $\mu$ depends on the thermal diffusivity $\alpha$ of the sample and the modulation rate $\omega$.

$$\mu = (2\alpha/\omega)^{1/2}.$$

The periodic diffusion process produces a periodic temperature fluctuation at the sample-gas interface. At a distance of $2\pi\mu_g$ (where $\mu_g$ is the thermal diffusion length in the gas), the periodic temperature change in the gas is effectively completely damped out. Only a boundary gas layer of thickness $2\pi\mu_g$ is then concerned in the PAS experiment. This boundary layer acts as a sinusoidally driven piston.

Assuming ideal gas behavior, Rosencwaig and Gersho obtained the following expression for the incremental pressure change as a function of time $\delta P(t)$:

$$\delta P(t) = Q \exp\,[i(2\pi\omega t - \pi/4)],$$

where $Q$ is a complicated expression specifying the complex envelope of the sinusoidal pressure variation. Fortunately, some special cases exist where the expression for $Q$ becomes relatively simple. Rosencwaig and Gersho grouped these cases according to the optical opaqueness of the solid as determined by

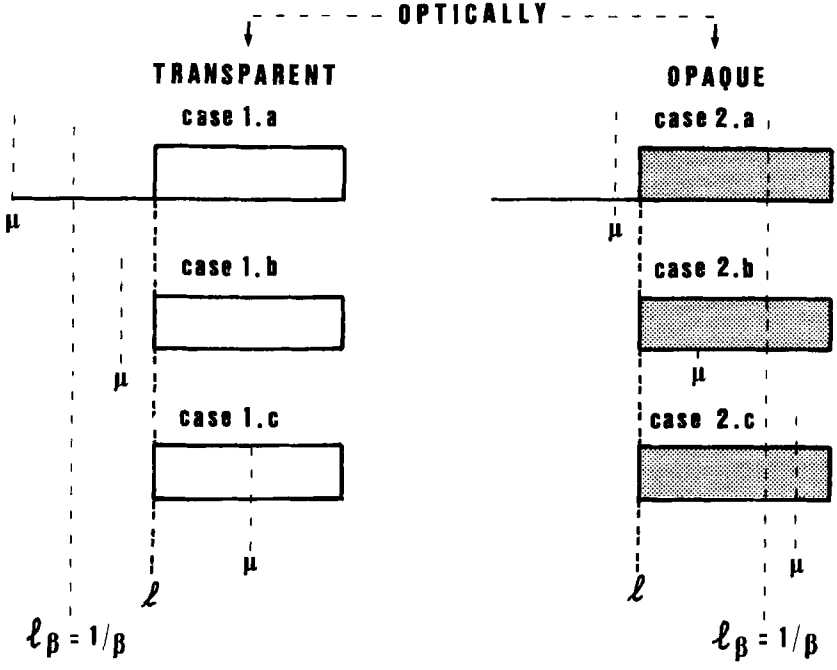


FIG. 3. Schematic representation of the different cases for the photoacoustic theory of solids (from Ref. 11).

the relation of the optical absorption length $l_\beta = 1/\beta$ to the thickness $l$ of the solid. Two cases were considered: optically transparent ($l_\beta > l$) and optically opaque ($l_\beta \ll l$) solids. For each category, three separate cases exist, based on the relationship between the thermal diffusion length $\mu_s$ of the sample, the physical length $l$, and the optical absorption length $l_\beta$. The six cases are shown in Fig. 3 and discussed below.

### A. Optically Transparent Samples ($l_\beta > l$)

In these cases the incident radiation is absorbed throughout the length of the sample. However, this does not mean that information will be attained from the entire sample since only heat originating from regions within one thermal diffusion length from the surface will be detected.

We define the following parameters:

$K$, the thermal conductivity ($cal \cdot cm^{-1} \cdot s^{-1} \cdot °C^{-1}$)
$\rho$, the density ($g/cm^3$)
$C$, the specific heat ($cal \cdot g^{-1} \cdot °C^{-1}$)
$\alpha = K/\rho C$, the thermal diffusivity ($cm^2/s$)
$a = (\omega/2\alpha)^{1/2}$, the thermal diffusion coefficient ($cm^{-1}$)
$\mu = 1/a$, the thermal diffusion length

We denote sample parameters by $s$, gas parameters by $g$, and backing material by doubly primed symbols.

*Case 1a.* Thermally thin samples ($\mu_s \gg l; \mu_s > l_\beta$). In this case $Q \simeq (1 - i)\beta l(\mu''/K'')Y/2a_g$, where $Y$ is a constant factor. The photoacoustic signal is proportional to $\beta l$, has a modulation dependence proportional to $\omega^{-1}$, and depends on the thermal properties of the backing material.

*Case 1b.* Thermally thick samples ($\mu_s > l; \mu_s < l_\beta$). For these types of samples, the expression for $Q$ is identical to Case 1a. The photoacoustic signal is proportional to $\beta l$, has a modulation dependence proportional to $\omega^{-1}$, and depends on the thermal properties of the backing material.

*Case 1c.* Thermally thick samples ($\mu_s < l; \mu_s \ll l_\beta$). In this case, $Q \simeq -i\beta\mu_s(\mu_s/K_s)Y/2a_g$. The signal is proportional to $\beta\mu_s$ rather than $\beta l$. Only the radiation absorbed within the first thermal diffusion length will generate a photoacoustic signal. The backing material (sample holder) does not contribute any signal even though radiation is being absorbed throughout the length $l$ of the sample. The frequency dependence of $Q$ varies as $\omega^{-3/2}$.

It is interesting to note that the frequency dependence of the acoustic signal gives the opportunity to obtain a depth profile of optical absorption within a sample. If the modulation frequency is very high, only information from the surface layers will be obtained. As the modulation rate is decreased, $\mu_s$ will increase and the spectrum will give information about the bulk of the sample.

### B. Optically Opaque Samples ($l_\beta \ll l$)

In these cases, most of the absorbed radiation is absorbed within a distance that is small compared to $l$, and very little radiation, if any, is transmitted.

*Case 2a.* Thermally thin samples ($\mu_s \gg l; \mu_s \gg l_\beta$). For these samples, $Q \simeq (1 - i)(\mu''/K'')Y/2a_g$. Photoacoustic as well as optical opaqueness can occur since the photoacoustic signal is independent of $\beta$. The signal depends on the thermal properties of the backing material and has a modulation dependence proportional to $\omega^{-1}$. This case is a particularly important one as it corresponds to carbon black which has very large values of $\alpha$ and $\beta$. This is why carbon black was proposed as a reference material for background spectra.

*Case 2b.* Thermally thick samples ($\mu_s < l; \mu_s > l_\beta$). In this case, $Q \simeq (1 - i)(\mu_s/K_s)Y/2a_g$. The expression for $Q$ is similar to the previous case, but the thermal parameters of the backing material are now replaced by those of the sample. The photoacoustic signal is independent of $\beta$ and varies as $\omega^{-1}$.

*Case 2c.* Thermally thick samples ($\mu_s \ll l; \mu_s < l_\beta$). For these samples, $Q \simeq -i\beta\mu_s(\mu_s/K_s)Y/2a_g$. This is a very interesting and important case. In the optical sense, the samples are very opaque solids ($\beta l \gg 1$), but as long as $\mu_s < 1$ (i.e., $\mu_s < l_\beta$), the samples are not photoacoustically opaque, and the light absorbed within the first diffusion length will generate a photoacoustic signal. This signal is proportional to $\beta$ and varies as $\omega^{-3/2}$.



## III. EXPERIMENTAL TECHNIQUES

From the experimental point of view, photoacoustic measurements are very easy to make. The first experiments on polymers were often performed with home-built cells, but photoacoustic cells are now commercially available. Such cells are often adaptable to the different existing FTIR spectrometers and may be purged for use of gases other than air in order to enhance the PA signal. Kinney and Staley [12] discussed some of the properties of suitable available gases. Helium is generally used as the fill gas on account of its superior thermal coupling properties. However, different gases have different thermal diffusion lengths, and one gas may be more suitable for use in one particular cell than in another. A discussion of cell design may be found in Ref. 9. Environmental noise around the equipment very often leads to a lower signal-to-noise ($S/N$) ratio. Duerst et al. [13, 14] proposed the use of an acoustically isolated chamber to enhance the $S/N$ ratio. Figure 4 illustrates the difference between two spectra of polypropylene obtained with and without such a chamber. It was concluded that the environmental room noise is a major contribution to poor $S/N$ ratios.

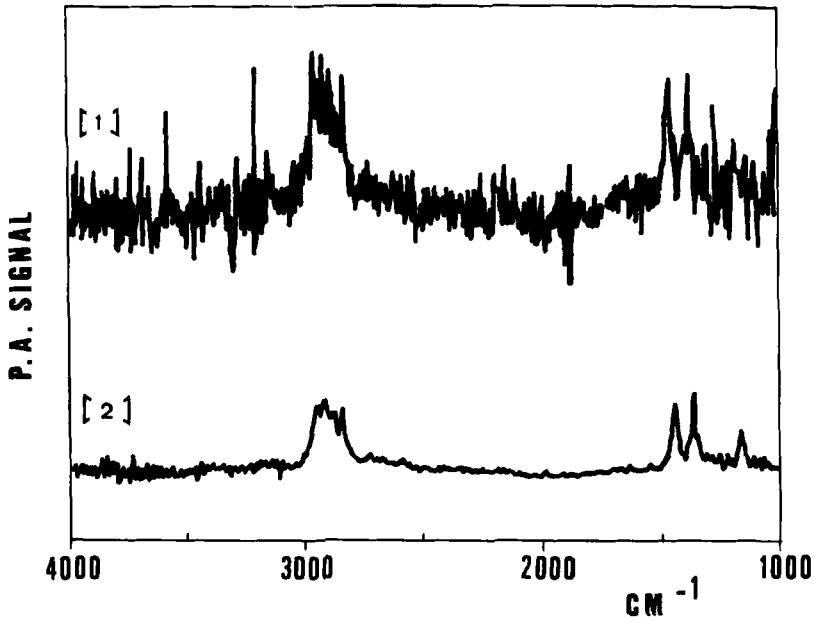


FIG. 4. PA spectrum of polypropylene: [1] without chamber, [2] with chamber (from Ref. 14).



### A. Sampling

A very attractive feature of infrared PAS is that no special sample preparation is needed. In fact, all the sample preparation problems encountered in transmission spectroscopy, such as interaction with KBr when making a salt pellet or changes of sample morphology, are avoided. However, particle size or surface morphology can substantially affect the PA spectrum. Yang and Fateley [15] studied the effect of particle size on FTIR-PAS by using naturally ground quartz. As shown in Fig. 5, the PAS peak intensities increase as the particle diameter decreases, and peak intensity ratios are not constant for particles of different diameters. Peak shape deteriorates with increasing particle size. When the particle diameter becomes smaller than the thermal diffusion length $\mu_s$ for a specific peak, a dramatic increase in peak intensity is observed. The effect of sample surface was examined by Vidrine [6] on samples of a commercially available plastic with different surface morphologies: powder, sawn surface, smooth surface, and pellets. The results are

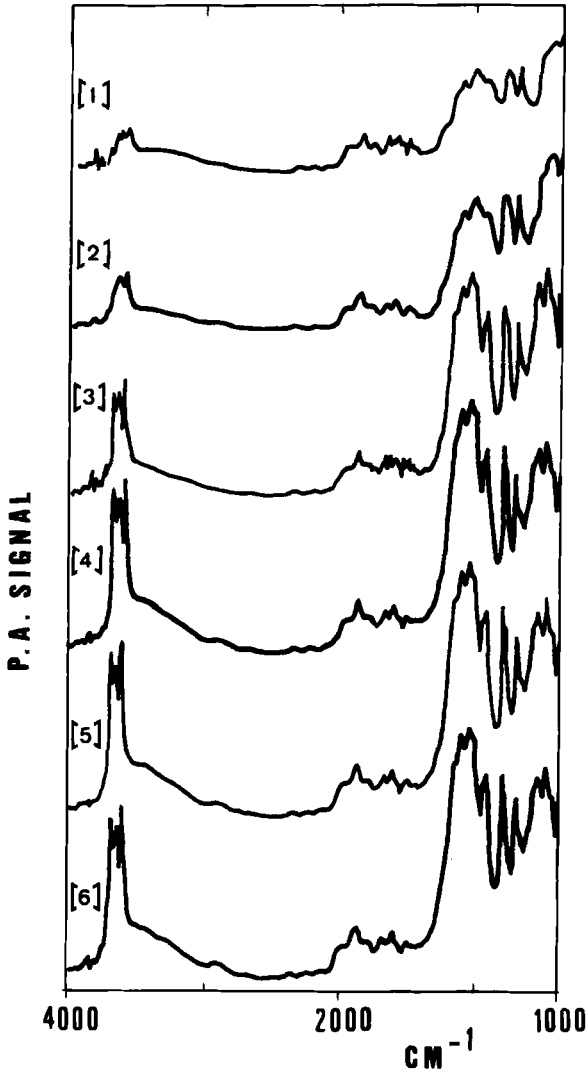


FIG. 5. PA spectrum of silica powder of different particle diameters: [1] 43-30 $\mu$m, [2] 30-20 $\mu$m, [3] 20-10 $\mu$m, [4] 10-5 $\mu$m, [5] 5-3.5 $\mu$m, and [6] 3.5-0 $\mu$m (from Ref. 15).

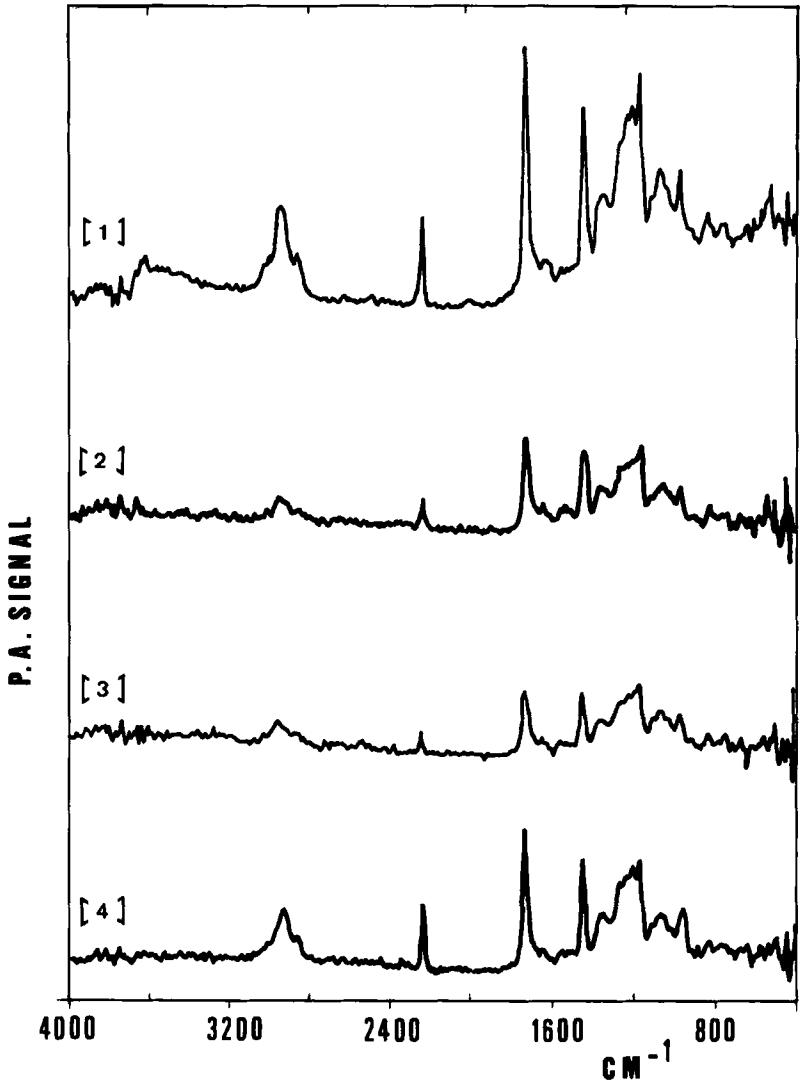


FIG. 6. PA spectra of a nitrile plastic with different surface morphologies: [1] powder, [2] sawn surface, [3] smooth surface, and [4] pellets (from Ref. 6).

shown in Fig. 6. The fine-powder sample produces the best spectrum because the efficiency of heat transfer from solid to gas is enhanced as the surface area/volume ratio increases.

Another important factor, pointed out by Teramae and Tanaka [16], is the effect of heat generated at the rear surface of a film sample on spectral features in FTIR-PAS. Figure 7 shows the spectra obtained with a bilayered polyethylene/poly(ethylene terephthalate) (PE/PET) film as a function of the sample position in a two-window PA cell. At the entrance window position, only the heat generated from the rear surface of the sample can contribute to the PA signal. When the sample is placed in the cell cavity, the heat

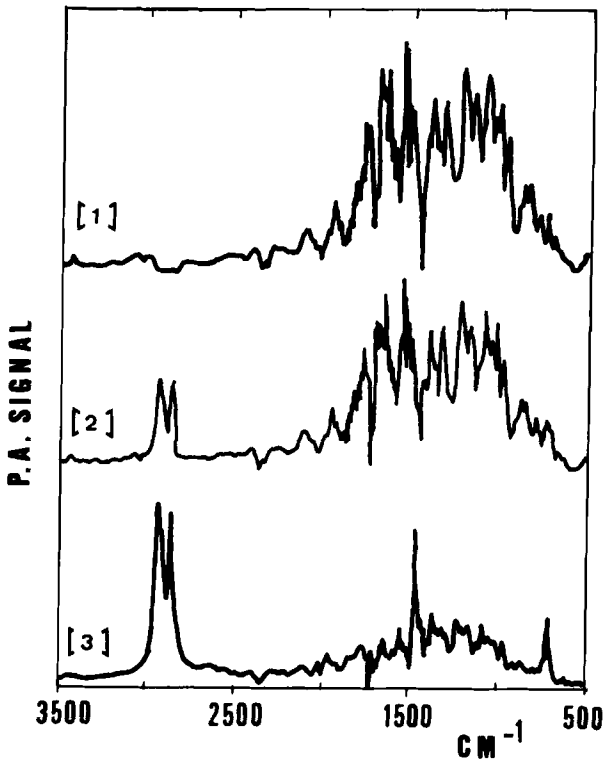


FIG. 7. PA spectrum of a bilayered PE/PET film with different positions in the PA cell: [1] at the entrance window, [2] in the middle of the cell, and [3] at the exit window (from Ref. 16).

generated from both the front and the rear surfaces can contribute to the PA signal. At the exit window position, only the heat from the front surface of the sample can contribute to the PA signal. Thus, when scanning the spectrum of a film-like sample, careful positioning of samples is required to eliminate the contribution from the heat generated at the rear surface. This can be done by adhesion of a suitable material to the rear surface.

### B. Normalization Procedures

In a FTIR-PAS experiment, the photoacoustic cell replaces the instrument detector. The cell output is processed by the electronics of the FTIR spectrometer to obtain the interferogram which may be Fourier transformed to yield an uncorrected absorption spectrum. The peak heights in this spectrum are not in the correct ratios for various reasons linked with the technique, and a normalization procedure must be used to obtain quantitative information.

Teng and Royce [17] discussed the different procedures that may be employed to obtain a quantitatively correct sample spectrum. FTIR spectrometers are single-beam instruments, and the PA signal is dependent on the spectral output of the infrared source modulated by the interferometer, and the observed peak heights must be corrected for the different energy output in different spectral regions. This correction is usually done by scanning a black absorber sample as the background. Different kinds of carbon black have been tested [9] as well as Fisher Norite. A decolorizing carbon is the recommended material for background spectra. Because carbon has a large capacity for $CO_2$ and $H_2O$ adsorption, some zeolite should be added to the chamber of the PA cell to remove contaminants from the gas in the cell and also from the carbon surface [17].

The effective modulation frequency $\omega$ of the infrared radiation incident on the PA cell is dependent on both the velocity of the moving mirror of the interferometer and the wavenumber, $\omega = 2\pi V\nu$, where $V$ is the optical velocity in cm/s and $\nu$ the frequency of the infrared source in wavenumbers. Because the thermal diffusion length $\mu_s$ depends on the modulation rate $\omega$, the PA spectrum will not be representative of a single depth but of a depth that varies linearly with wavelength. If a different mirror velocity $V'$ is chosen, the frequency $\omega'$ associated with a given wavenumber $\nu$ will change: $\omega' = 2\pi V'\nu$.

Teng and Royce [17] described a method of correction for a PA spectrum scanned at two different mirror velocities. Figure 8 shows the result obtained with a poly(methyl methacrylate) (PMMA) sample. More recently, Graham et al. [9] proposed a correction that uses a spectrum scanned at only one mirror velocity.

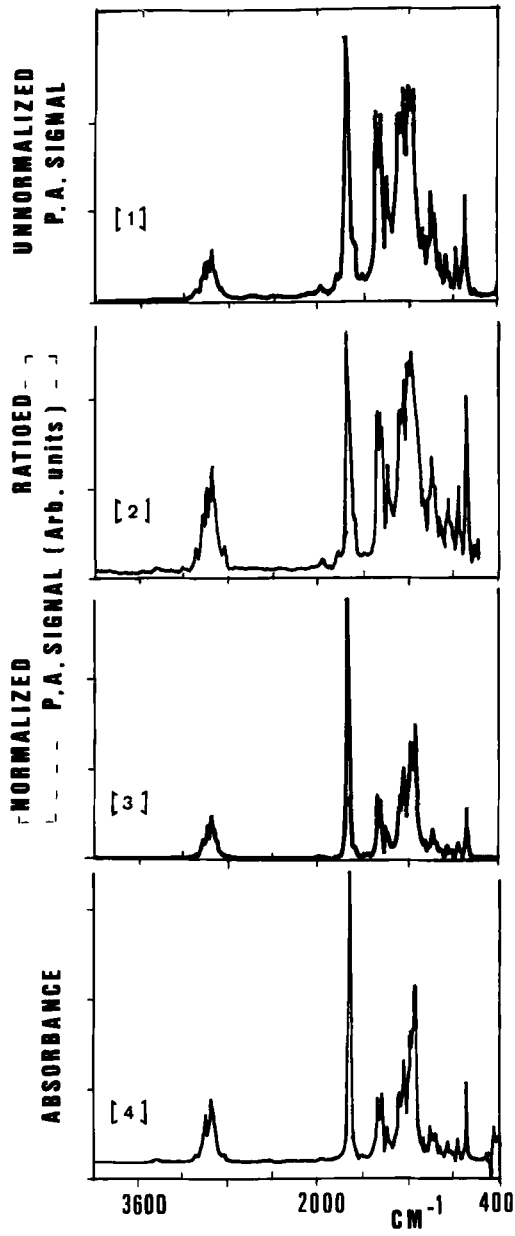


FIG. 8. Effect of normalization procedures on the PA spectrum of poly-(methyl methacrylate): [1] uncorrected spectrum, [2] spectrum corrected for the different energy output, [3] normalized PA spectrum, and [4] transmission spectrum (from Ref. 17).

### C. Fourier Self-Deconvolution of Photoacoustic FTIR Spectra

Infrared spectra of polymers very often consist of peaks that overlap extensively, making quantitative analysis difficult. An interesting method to increase the apparent resolution of spectra through deconvolution in Fourier space was proposed by Kauppinen et al. [18]. In this technique the inverse Fourier transform of the spectrum $E(\nu)$ to be deconvoluted, $I(x) = \mathbf{F}^{-1}[E(\nu)]$, is multiplied by a function $D(x)/\mathbf{F}^{-1}[E_0(\nu)]$, where $D(x)$ is an apodization function and $E_0(\nu)$ is the intrinsic line-shape function of the spectrum $E(\nu)$. The self-deconvoluted spectrum $E'(\nu)$ is then the Fourier transform of the new interferogram $I'(x)$. Friesen and Michaelian [19] demonstrated that the photoacoustic interferogram can be used directly without the usual intermediate computation of the spectrum. Phase errors in the interferogram must be eliminated as a first step of the calculation. The usual procedure is then applied. An example of a coal self-deconvoluted spectrum in the aliphatic C–H region is shown in Fig. 9. The resolution enhancement is quite clear and reveals a considerable amount of structure.



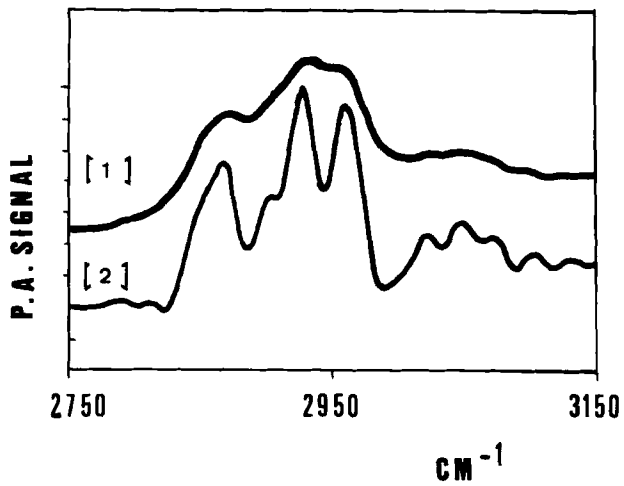


FIG. 9. Coal: [1] PA spectrum in the 2750 to 3150 $cm^{-1}$ range, [2] self-deconvolution (from Ref. 19).

## IV. EXPERIMENTAL RESULTS

FTIR-PAS is mainly a surface stpectroscopic analysis. One of its greatest advantages is that it overcomes experimental difficulties such as air/or water sensitivity, insolubility, infusibility, and opacity. The following examples demonstrate the utility of this technique.

Characterization of different textile fabrics was performed by FTIR-PAS. Cotton and poly(hexamethylene adipamide) [20] were clearly identified. In textile mixtures of wool/polyester and of wool/polyamide/cellulosic material, the spectra of the different components were isolated by a subtraction process [21].

Information about the curing of a resol-type phenolic resin was obtained by Teramae et al. [22]. As the resin was heated, the intensity of the band due to C–O–C stretching vibrational mode at about 1050 $cm^{-1}$ decreased and a new band, due to the carbonyl stretching vibrational mode at about 1550 $cm^{-1}$, appeared. This band was tentatively assigned to the oxidation of methylene groups. These authors compared the results obtained by PAS with spectra run by a KBr transmission technique. The two sets of results provide similar results for the curing curves. However, some differences for the extent of curing were noted between the surface and the bulk sample. In the same paper, FTIR-PAS spectra of butadiene-acrylonitrile rubbers containing up to 20% of carbon black are also presented.

FTIR-PAS was also used to obtain the infrared spectra of conducting polymers. When doped, such samples are easily destroyed by exposure to oxygen. As the PA cell can be easily purged with an inert gas such as argon, it is ideally suited for these types of samples. The spectra of undoped, *n*-doped [23], and *p*-doped [24] polyacetylene, as well as polyparaphenylene and its derivatives [25], were obtained by this method.

Since FTIR-PAS is mainly concerned with the surface of the sample, it presents a very attractive tool for examination of chemical modifications on the surface of polymers. Furthermore, spectral subtraction allows one to enhance the effect of the chemical treatment. In a study of plasma-oxidized poly(styrene-*co*-divinylbenzene) beads, Gerson [26] observed the appearance of strong absorption bands at 1724 and 1693 $cm^{-1}$, characteristic of carbonyl groups, and at 1245, 1177, and 1103 $cm^{-1}$, characteristic of ester/ether linkages, which indicate that the copolymer surface was highly oxidized in the treated sample (Fig. 10). Dehydrofluorination of poly(vinyl fluoride) films [27] and chemical modification of poly(ethylene terephthalate) fibers [28] have also been investigated.

The same technique was applied by Chatzi et al. [29] to determine the

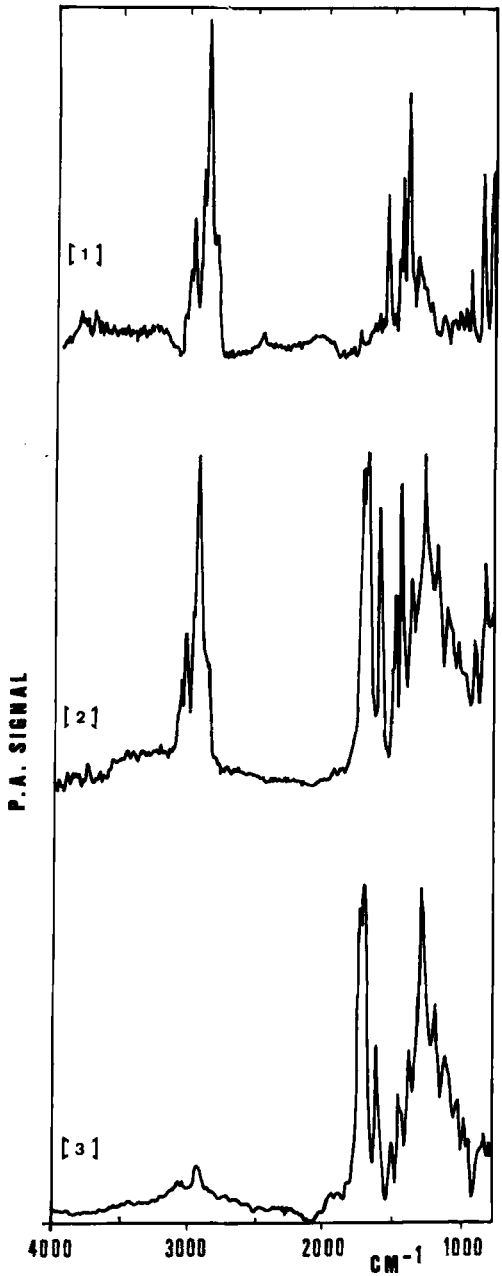


FIG. 10. PA spectrum of poly(styrene-*co*-divinylbenzene) beads: [1] unoxidized polymer, [2] oxidized polymer, and [3] difference spectrum, oxidized minus unoxidized (from Ref. 26).

accessibility of N–H groups of poly(*p*-phenylene terephthalamide) fibers for deuterium exchange. It was shown that 70% of the N–H groups belongs to highly ordered inaccessible material. Heat treatment at 150°C for 2 h results in a 43% decrease of the originally accessible material due to an improvement of the molecular packing.

Orientation is often introduced in plastic materials to improve their physical properties. Thus, there is a great deal of interest in the molecular phenomena which occur during stretching or any forming process. Vibrational spectroscopy is a very valuable tool for measuring molecular processes occurring in the bulk [30], and FTIR-PAS should allow one to determine the surface orientation of polymer samples. Krishnan et al. [31] showed that dichroic spectra of excellent quality can be obtained by the PA method. The polarized PA spectra of a uniaxially drawn poly(ethylene terephthalate) sheet were recorded by using a gold wire grid polarizer and compared with polarized ATR spectra. Figure 11 shows the two polarized PA spectra of PET. The dichroic ratios obtained by PAS are lower than those obtained by ATR. This fact was related to the difference of depth of penetration of the infrared beam between the two sets of experiments. Indeed, according to Krishnan [32], the depth of penetration is greater in the PA experiments than in the ATR experiments. In hot-rolled PET samples the surface may be expected to be more oriented than the bulk, and greater dichroic ratios should be measured by ATR as is observed experimentally. It is interesting to note that PAS can be used to determine orientation in samples that are strongly absorbant or have rough or brittle surfaces.

On the other hand, Urban and Koenig [33] proposed an interesting PAS method to obtain useful information on surface functionality and adsorbed species by using a highly polarizable coupling gas in the PA cell and comparing the spectra to others obtained with a nonpolarizable coupling gas. A highly polarizable gas, such as xenon, enhances those surface modes which are preferentially oriented parallel to the surface and suppresses the intensity of the perpendicular modes. This technique was first applied to the adsorption of water and carbon monoxide on silica surfaces [33], preferentially reflecting perpendicular orientation of hydroxyl groups with respect to the surface. Similarly, the same authors studied the orientation of silanes on silica surfaces [34]. Silanes are widely used as coatings on glass fibers in composite materials. Because the structure of the fiber-matrix interface strongly influences the properties of the final products, it is interesting to obtain information on the local structure of silanes at the interface. It has been shown that the type of orientation is a function of the extent of surface coverage. At low surface coverage, coupling agents tend to take a perpendicular orientation with respect to the surface, and increasing surface coverage leads to parallel

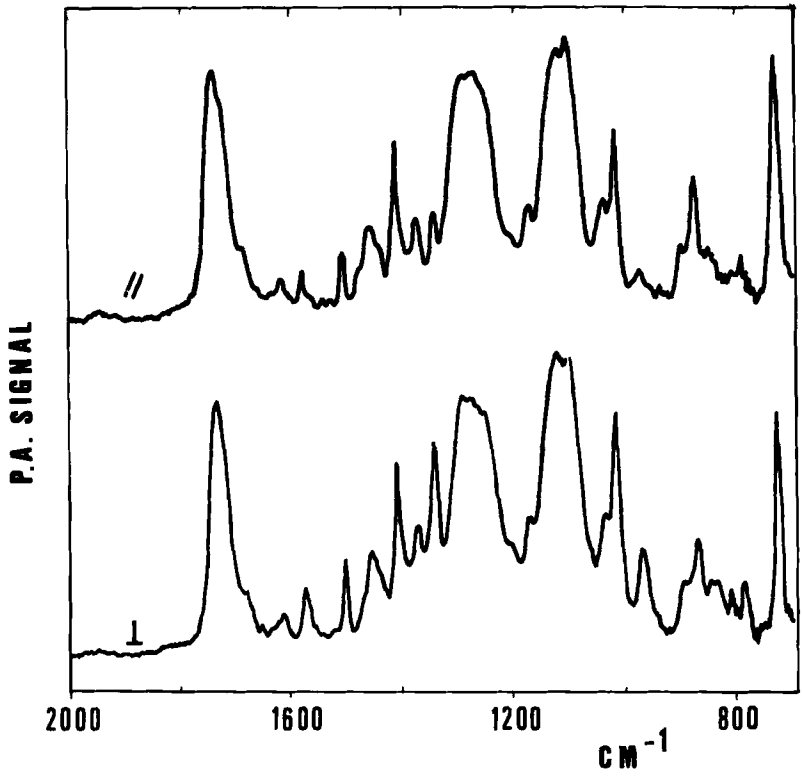


FIG. 11. Polarized PA spectra of PET surface (from Ref. 31).



orientation. Increasing the coupling agent concentration also induces orientational changes of hydroxyl, water, and carbonyl groups which form chemical bonds with the silica surface. The same method has also been applied to the characterization of poly(*p*-phenylene terephthalamide) fiber surfaces [35]. Differences in the structure of the skin and the core of the fibers were pointed out. The polymer chains in the skin are oriented parallel to the surface, and they are almost radially oriented in the core.

As we have seen before, FTIR-PAS is an interesting technique for surface analysis of polymer compounds. A very attractive feature is the possibility of varying the sampling depth by changing the modulation frequency, i.e., the mirror velocity of the interferometer. An illustration of the magnitude of PA signal as a function of frequency for a sample of pressed Si powder

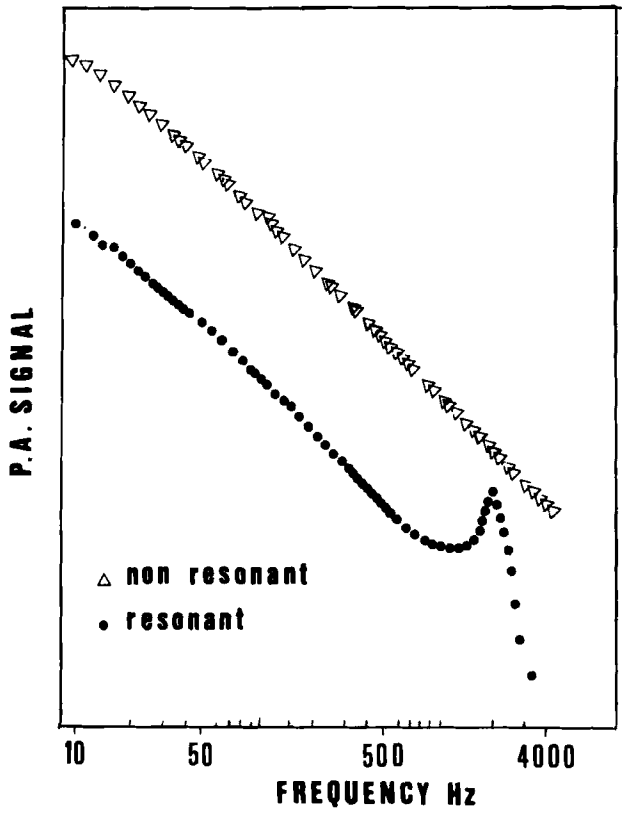


FIG. 12. Magnitude of PA signal as a function of frequency for a sample of pressed Si powder for nonresonant and resonant cells (from Ref. 36).



for nonresonant and resonant cells is shown in Fig. 12. By using a higher mirror velocity to achieve a smaller effective measurement depth, a significant decrease in the signal-to-noise ratio is observed if modulation frequencies above the cell resonance frequency are used. This fact imposes a lower limit of a few micrometers on attainable effective penetration depths. A comparison of attenuated total reflectance (ATR) and PAS for surface analysis of biocompatible polymer mixtures was published by Gardella et al. [37]. The bulk composition of these biocompatible polymers is as follow; the first one was a polyether [poly-(tetramethylene oxide)] and polyurethane mixture (toluene-2,4-diisocyanate and ethylenediamine chain extender), while the second one was a mixture of

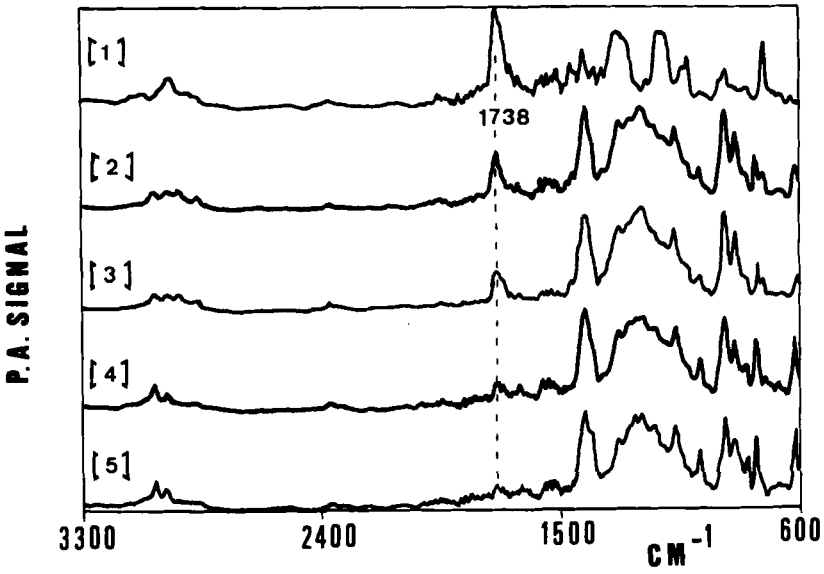


FIG. 13. PA spectra of PVDF-on-PET films with various PVDF thicknesses (mirror velocity: 0.3 cm/s): [1] PET, [2] PVDF (3 μm)-on-PET, [3] PVDF (6 μm)-on-PET, [4] PVDF (9 μm)-on-PET, and [5] PVDF (12 μm)-on-PET (from Ref. 39).



poly(dimethylsiloxane) and a polyether[poly(propylene glycol)]-polyurethane-(toluene-2,4-diisocyanate and 1,4-butanediol chain extender) structure. Results from the analysis of these two mixtures and their homopolymer constituents allowed the detection of surface impurities and segregation of specific polymer components in a region near the surface.

In a study of PS-on-PMMA films of different thicknesses [38], it was shown that ATR reaches to a depth of less than 2 μm, while the PAS analytical depth extends to 15-20 μm. These values are dependent upon the optical and thermal properties of the sample; however, these general trends are thought to be applicable to optically transparent, thermally thick polymer thin films. In a recent paper, Urban and Koenig [39] evaluated the penetration of infrared light in a PET film by recording the PA spectra of four different thicknesses of poly(vinylidene difluoride) (PVDF) on PET at a mirror velocity of 0.3 cm/s. As shown in Fig. 13, the carbonyl band of PET at 1738 $cm^{-1}$ is minimal at a thickness of 12 μm, which corresponds to the depth of penetration in PET.

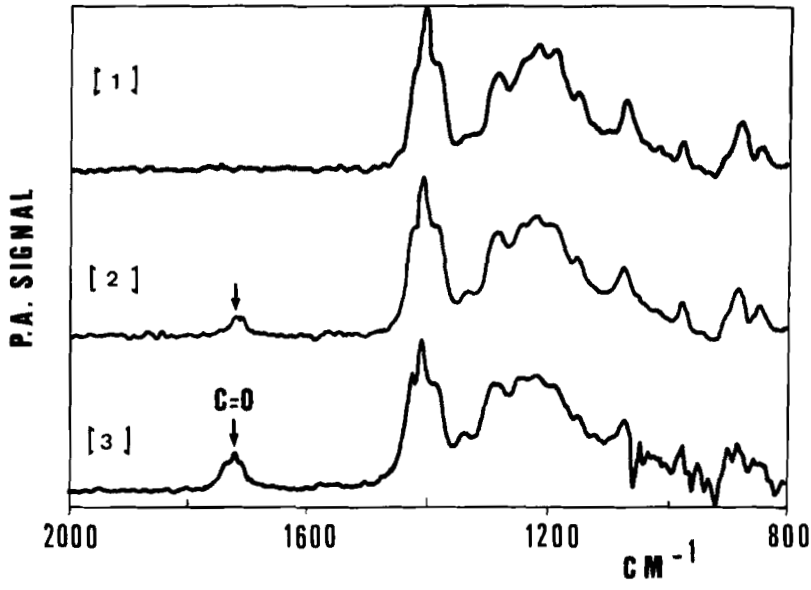


FIG. 14. PA spectra of a 12-$\mu$m overlayer of PVDF-on-PET scanned at different mirror velocities: [1] 0.6 cm/s, [2] 0.3 cm/s, and [3] 0.15 cm/s (from Ref. 39).

As shown in Fig. 14, changing the mirror velocity from 0.5 to 0.15 cm/s results in the appearance of the strong carbonyl band of PET at 1738 $cm^{-1}$. The intensity of this band diminishes as the mirror velocity increases, and further increases lead to complete disappearance of the band. A plot of the intensities of the carbonyl absorption band as a function of mirror velocity indicated an $\omega^{-3/2}$ dependence, in agreement with theoretical predictions for thermally thick and optically transparent samples (Case 1c).

Another analysis of multilayered films was performed by Teramae and Tanaka [40]. In this study the spectrometer operated at a single fixed mirror velocity. Spectral separation of the subsurface layer was carried out by subtraction of PA spectra of bilayered films with a top layer of various thicknesses. The spectrum of the subsurface layer could then be isolated.

The chemical changes within measurable surface layers of solid samples were investigated by Yang et al. [41]. In this study, sized cotton yarns, treated glass fibers, chemically modified poly(ethylene terephthalate) fibers,

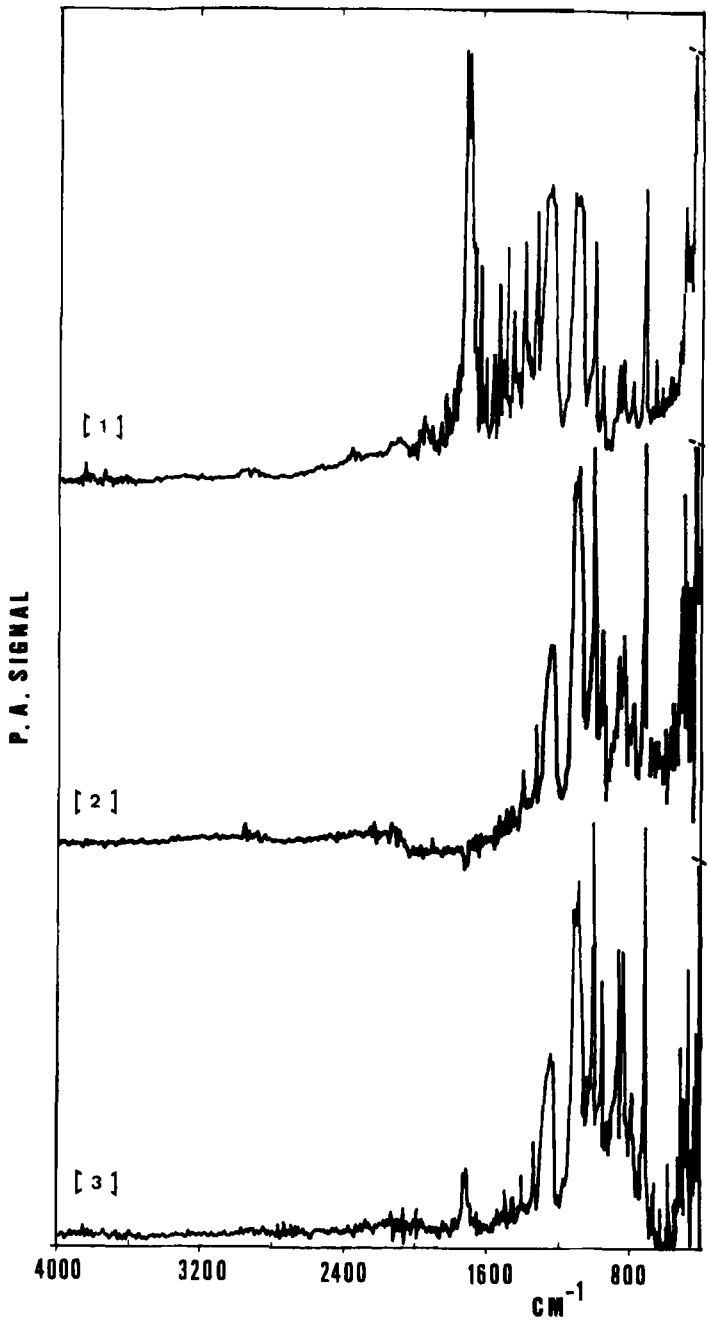


FIG. 15. PA spectrum of PET at different mirror velocities: [1] 0.220 cm/s, [2] 0.470 cm/s, and [3] 0.503 cm/s (from Ref. 13).

and a naturally weathered poly(vinyl chloride) (PVC) composite were studied by FTIR-PAS at different mirror velocities. It was shown that a polyacrylate sizing agent exhibits better penetration in cotton yarn than a polyurethane sizing agent. In PET fibers treated with a block copolymer, the finish is more concentrated in a surface layer 1.5 $\mu$m thick than in the underlying layers, and in weathered PVC, hydrolysis and oxidization are a near-surface phenomenon.

All these studies confirm that FTIR-PAS can be successfully applied to depth profiling studies of multilayer films which are of particular interest for packaging and other applications. However, in performing these spectroscopic studies, one must always be cautious of the phenomenon known as phase-lag. As a matter of fact, the heat liberated by the sample in PAS must first be transported through the sample. This allows the surface-generated heat to be detected before the bulk-generated heat, and a time delay exists between the detection of these two generated heats. A phase error in the Fourier transform spectrum will occur whenever the phase difference between the two generated heats becomes too large for the Fourier-transform phase correction routine to handle. The phase error produces an asymmetrical peak, and an inversion of the peak is observed if the phase error reaches 180°. The general features all along the spectrum usually remain unchanged as the modulation rate increases. This, however, is not true for the strongly absorbing carbonyl band. In a depth-profiling study of 50 $\mu$m thick PET film [13], spectra were taken with mirror velocities from 0.176 to 0.640 cm/s. As shown in Fig. 15, a "negative" carbonyl band at 1730 $cm^{-1}$ is observed for a mirror velocity of 0.47 cm/s. Similarly, Graham et al. [9] observed a fairly large phase error in a five-layer laminar polymer film. However, these authors suggest that, by correcting for the phase error as a function of wavenumber and modulation rate, it should be possible to successfully depth-profile a sample.



## REFERENCES

[1] A. G. Bell, *Am. J. Sci., 20,* 305 (1880).
[2] A. G. Bell, *Philos. Mag., 11,* 510 (1881).
[3] A. Rosencwaig, *Opt. Commun., 7,* 305 (1973).
[4] M. G. Rockley, *Chem. Phys. Lett., 68,* 455 (1979).
[5] M. G. Rockley, *Appl. Spectrosc., 34,* 405 (1980).
[6] D. W. Vidrine, *Ibid., 34,* 314 (1980).
[7] D. W. Vidrine and S. R. Lowry, in *Polymer Characterization* (C. D. Craver, ed.), (Advances in Chemistry Series 203), American Chemical Society, 1983, p. 595.

[8] J. L. Koenig, *Adv. Polym. Sci., 54,* 87 (1983).
[9] J. A. Graham, W. M. Grim III, and W. G. Fateley, in *Fourier Transform Infrared Spectroscopy,* Vol. 4 (J. H. Ferraro and L. J. Basile, eds.), Academic, 1985, p. 345.
[10] A. Rosencwaig and A. Gersho, *Science, 190,* 556 (1975); *J. Appl. Phys., 47,* 4 (1976).
[11] A. Rosencwaig, *Photoacoustics and Photoacoustic Spectroscopy,* Wiley, 1980.
[12] J. B. Kinney and R. H. Staley, *Anal. Chem., 55,* 343 (1983).
[13] R. W. Duerst, P. Mahmoodi, and M. D. Duerst, in *Fourier Transform Infrared Characterization of Polymers* (H. Ishida, ed.), Plenum, 1987, p. 113.
[14] P. Mahmoodi, R. W. Duerst, and R. A. Meikle-John, *Appl. Spectrosc., 38,* 437 (1984).
[15] C. Q. Yang and W. G. Fateley, *J. Mol. Struct., 146,* 25 (1986).
[16] N. Teramae and S. Tanaka, *Anal. Chem., 57,* 95 (1985).
[17] Y. C. Teng and B. S. Royce, *Appl. Opt., 21,* 77 (1982).
[18] J. K. Kauppinen, D. J. Moffat, H. H. Mantsch, and D. G. Cameron, *Appl. Spectrosc., 35,* 271 (1981).
[19] W. I. Friesen and K. H. Michaelian, *Infrared Phys., 26,* 235 (1986).
[20] N. Teramae and S. Tanaka, *Spectrosc. Lett., 14,* 687 (1981).
[21] R. S. Davidson and G. V. Fraser, *J. Soc. Dyers Colour., 100,* 167 (1984).
[22] N. Teramae, M. Hiroguchi, and S. Tanaka, *Bull. Chem. Soc. Jpn., 55,* 2097 (1982).
[23] S. M. Riseman, S. I. Yaniger, E. M. Eyring, D. Macinnes, A. G. Macdiarmid, and A. Heeger, *Appl. Spectrosc., 35,* 557 (1981).
[24] S. I. Yaniger, S. M. Riseman, T. Frigo, and E. M. Eyring, *J. Chem. Phys., 76,* 4298 (1982).
[25] S. I. Yaniger, D. J. Rose, W. P. McKenna, and E. M. Eyring, *Appl. Spectrosc., 38,* 7 (1984); *Macromolecules, 17,* 2579 (1984).
[26] D. J. Gerson, *Appl. Spectrosc., 38,* 436 (1984).
[27] E. M. Salazar-Rojas and M. W. Urban, *Polym. Prepr., 28,* 1 (1987).
[28] C. Q. Yang, J. F. Moulder, and W. G. Fateley, *Ibid., 28,* 3 (1987).
[29] E. G. Chatzi, M. W. Urban, H. Ishida, and J. L. Koenig, *Polymer, 27,* 1850 (1986).
[30] B. Jasse and J. L. Koenig, *J. Macromol. Sci.–Rev. Macromol. Chem., C17,* 61 (1979);
[31] K. Krishnan, S. Hill, J. P. Hobbs, and C. S. P. Sung, *Appl. Spectrosc., 36,* 257 (1982).
[32] K. Krishnan, *Ibid., 34,* 549 (1981).

[33] M. W. Urban and J. L. Koenig, *Ibid., 39,* 1051 (1985).
[34] M. W. Urban and J. L. Koenig, *Ibid., 40,* 513 (1986).
[35] E. G. Chatzi, M. W. Urban, and J. L. Koenig, *Makromol. Chem., Makromol. Symp., 5,* 99 (1986).
[36] G. Benedetto, M. Maringelli, and R. Spagnolo, *Rev. Sci. Instrum., 58,* 975 (1987).
[37] J. A. Gardella, G. L. Grobe III, W. L. Hofson, and E. M. Eyring, *Anal. Chem., 56,* 1169 (1984).
[38] D. A. Saucy, S. J. Simko, and R. W. Linton, *Anal. Chem., 57,* 871 (1985).
[39] M. W. Urban and J. L. Koenig, *Appl. Spectrosc., 40,* 994 (1986).
[40] N. Teramae and S. Tanaka, *Ibid., 39,* 797 (1985).
[41] C. Q. Yang, R. R. Bresee, and W. G. Fateley, *Ibid., 41,* 889 (1987).